AIAA JOURNAL
Vol. 39, No. 2, February 2001

Response of Simple Turbulence Models to Step Changes of Slip Velocity

Irina Bassina* and Mikhail Strelets†
Federal Scientific Center "Applied Chemistry," 197198, St. Petersburg, Russia
and
Philippe R. Spalart‡
The Boeing Company, Seattle, Washington 98124-2207

A numerical study was performed of two turbulent boundary layers with sudden changes of the slip velocity at the wall. The first is the two-dimensional flow on a flat plate with a sudden increase of the wall velocity. The second flow is a three-dimensional boundary layer along a cylinder whose upstream section is rotating with a constant circumferential velocity, while the downstream section remains still. Computations were carried out with a wide range of simple eddy-viscosity models: an algebraic model, two one-equation models, a two-equation k–ε model, and a zonal k–ω model. For the two-dimensional flow, it is shown that though all of the models somewhat overestimate the rate of relaxation of the inner region of the boundary layer after its perturbation, they are quite capable of predicting the crucial reduction in skin friction over the moving wall. They also describe adequately the insensitivity of the outer region of the boundary layer to the removal of the inner region, found in the experiments. From the standpoint of accuracy of the major two-dimensional flow characteristics, the zonal k–ω and two one-equation models appear to be close to each other and significantly better than the two-equation k–ε and algebraic models. For the three-dimensional flow, all of the models perform approximately equally, with only a slight superiority of the differential models over the algebraic model. When one considers that these models cannot reproduce the significant deviation between the Reynolds-stress vector and the shear vector observed in the experiment, the agreement of the computations with the data on the mean flow characteristics is unexpectedly good.

Introduction

A LARGE change of the solid wall velocity results in a significant alteration of the turbulent boundary-layer structure, independent of pressure gradients. It could constitute a severe test for turbulence models, which are designed and calibrated mostly with zero slip velocity. Even if the models fail to predict the effect accurately, it is of interest to find out how different models compare, which can give guidelines for their improvement. These tests can be performed using the boundary-layer equations.

Several experimental studies are available where an abrupt change of the wall velocity is obtained (for instance, see Refs. 1–4). In the present work we have computed two of them,[1,2] both being relatively simple but representative enough to provide an answer to the question of whether eddy-viscosity models are capable of predicting consistently the major effects observed in the experiments.

In the experiments by Hamelin and Alving (H–A),[1] a sudden change of the slip velocity under the canonical turbulent boundary layer on a stationary flat plate is obtained by translating a section of the wall underneath the boundary layer in the direction of the mean flow, using a belt (see schematic Fig. 1a). It results in the sudden removal of the inner part of the layer, which represented about 60% of the velocity difference, providing insight into the interaction between this inner high-shear region and the outer regions of the turbulent boundary layer. The elucidation of that interaction mechanism is both of scientific interest and of practical importance because most of the semi-empirical turbulence models are, explicitly or implicitly, based on the two-layer turbulent boundary-layer concept. Thus, a better understanding of the inner–outer interaction may greatly help the enhancement of such models.

The second flow chosen as a benchmark in the present work was studied experimentally by Driver and Hebbar (D–H)[2] in 1987. Just as with the H–A flow, it involves a sudden change of the slip velocity, but of a quite different nature. Namely, D–H studied the decay of crossflow on a stationary section of cylinder located immediately downstream of a spinning section (see schematic Fig. 1b). In this three-dimensional boundary layer, just as in the two-dimensional H–A case, the memory effects, of which the correct prediction with simple turbulence models is doubtful, might play an important role. In addition, a peculiar feature of the D–H boundary layer is a rapid change in mean rate of strain along the streamlines resulting in significant Reynolds-stress anisotropy. Therefore, the D–H flow seems to be a challenging test, particularly for turbulence models based on the scalar eddy-viscosity assumption.

Numerical Technique and Problem Statement

Computations were performed using a plane-two-dimensional/axisymmetric-three-dimensional turbulent boundary-layer solver. It implements an implicit two-layer finite difference scheme of the first order in the x direction, streamwise, and a second-order scheme in the y direction. The grid is nonuniform in both directions with x clustering in the region of the sudden change of slip velocity (near the beginning of the moving belt for the H–A flow and in the vicinity of the junction of the spinning and still cylinders for the D–H flow) and with y clustering near the wall. At every streamwise step the finite difference equations are solved by the scalar tridiagonal matrix inversion algorithm, with iterations for the nonlinear terms.

Boundary conditions are as follows. The streamwise velocity at the outer edge of the boundary layer, U_e, is generally used for normalization. The freestream boundary conditions for the turbulent characteristics needed for the turbulence transport equations of the differential turbulence models, reproduce the low-turbulence level (0.1%) in the experiment. For the eddy-viscosity transport equations [the Spalart–Allmaras (S–A)[5] model and Shur et al.[6] ν_t-92 model], it is reached by setting the eddy viscosity ν_{te} at the outer edge of the boundary layer to 10^{-3} times the molecular viscosity ν. For the Chien[7] k–ε and Menter[8] k–ω (M-SST) models, the turbulence energy k_e at the outer edge is set to the experimental value $10^{-6}\ U_e^2$, and the value of ε_e is computed by the already mentioned ν_{te} and k_e values. For the specific dissipation rate ω_e, the following relation recommended in Ref. 8 is used:

Received 23 September 1997; revision received 6 June 2000; accepted for publication 6 June 2000.

*Senior Research Scientist, Computational Fluid Dynamics Group.
†Principal Scientist, Computational Fluid Dynamics Group.
‡Technical Fellow, Commercial Airplanes Group.

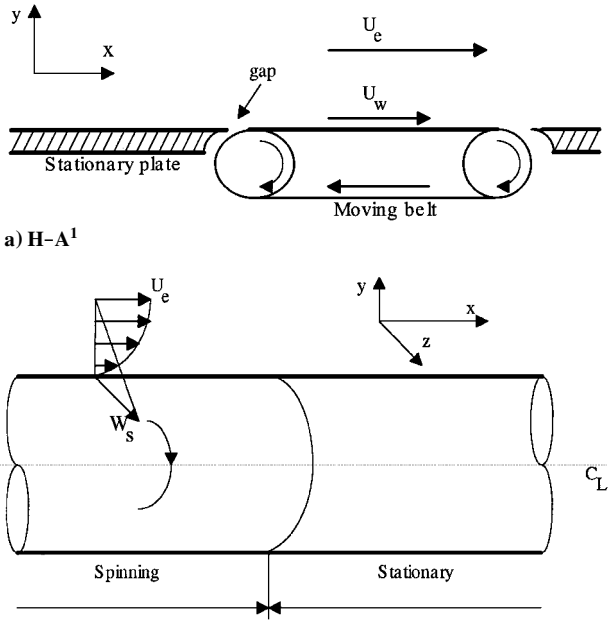

Fig. 1 Schematic of the experimental setup.

$$\omega_e = \frac{4 \cdot u_*^2}{(\beta^*)^{\frac{1}{2}} U_e \delta^*}$$

where the friction velocity is $u_* = (\tau_w/\rho)^{1/2}$, δ^* is the boundary-layer displacement thickness, and $\beta^* = 0.09$.

Note that, based on Ref. 9 and our own sensitivity study, the considered models are not sensitive to the parameters of the freestream turbulence and, particularly, do not react to two orders of magnitude increase or decrease vs the values pointed out earlier.

At the stationary part of the solid wall, the boundary conditions for the momentum equation are the conventional no-slip and nonpermeability conditions. At the moving belt, the streamwise velocity is set to that of the belt, that is, 4 m/s compared with $U_e = 6.5$ m/s, and downstream of the belt, it is set to zero again.

Special attention should be paid to the boundary conditions at the gap between the stationary plate and the moving belt. The belt drags additional fluid into the boundary layer. In Ref. 1 the mass flux of that injected fluid is estimated to be approximately 1% of the mass flux across the boundary layer. To model this effect, the boundary conditions at the gap are imposed as follows. The streamwise velocity is assumed to vary linearly from zero at the end of the stationary plate up to the belt velocity at the end of the gap, the length of which is estimated as 0.02 m. The normal velocity component over the gap, v_w, is assumed constant and computed to match the earlier value of the injected mass flux (1% of the mass flux across the boundary layer). It gives a value of $v_w = 0.097$ m/s. To assess the sensitivity of the flow to v_w, runs were performed also with $v_w = 0$ and with $v_w = 0.291$ m/s.

The wall boundary conditions for ν_t, k, and ε are zero, and the wall value of the specific dissipation rate, ω_w, is computed as in Ref. 8:

$$\omega_w = \frac{10 \cdot 6\nu}{\beta_1^2 \Delta y_w}, \qquad \beta_1 = 0.0750$$

where ν is the molecular kinematic viscosity and Δy_w is the near-wall grid step.

Finally, the inflow profiles, at the leading edge of the stationary plate, are assumed uniform for all of the flow quantities. In the experiments,[1] a fixed transition location is obtained by a wire located at the start of the test section. Thus, in our computations all of the turbulence models were activated in the very beginning of the stationary plate. For the algebraic Cebeci–Smith (C–S) model (see Ref. 10), this is straightforward (by switching the model on at $x = 0.15$ m downstream of the plate beginning). For the differential models, transition is controlled by means of special trip terms introduced in the corresponding transport equations by analogy with

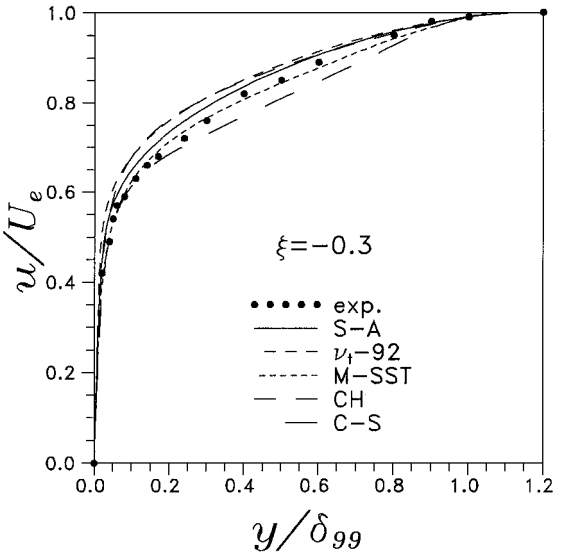

Fig. 2a Computed and measured streamwise mean velocity profiles at $\xi = -0.3$.

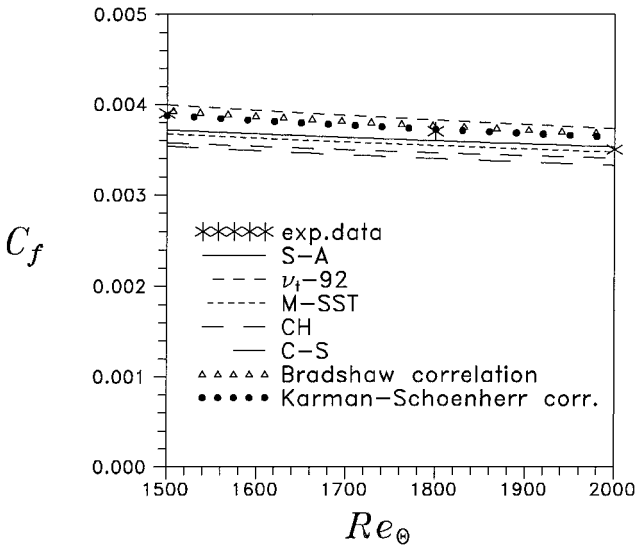

Fig. 2b Skin-friction coefficient distributions along the stationary plate.

that term in the S–A model.[5] In all of the cases it results in a fast transition to turbulence at the stationary plate and in the formation of a turbulent boundary layer with its main characteristics close to those in the experiment (see Figs. 2 and 3).

For the D–H flow, the only difference is that the circumferential velocity on the spinning section is $W_s = U_e = 36$ m/s. The computations were started near the end of the spinning cylinder, at $x = -5\delta_0$ ($\delta_0 = 0.029$ m is the boundary-layer thickness at the first experimental section). The experimental velocity components u and w and turbulent kinetic energy k distributions measured at that section in the experiment, along with the experimental data on the eddy viscosity ν_t, were directly used as the corresponding inlet boundary conditions. The inlet profiles of ω and ε needed for the M-SST and Chien models were computed with the use of the experimental data on k and ν_t.

Grid-refinement studies were conducted for both flows with all of the turbulence models, and the grid parameters were chosen providing the virtually grid-independent solutions discussed in the next section.

Results and Discussion

H–A Flow

Figure 2a shows the agreement between the models' predictions and experimental data on the streamwise mean velocity profile at the

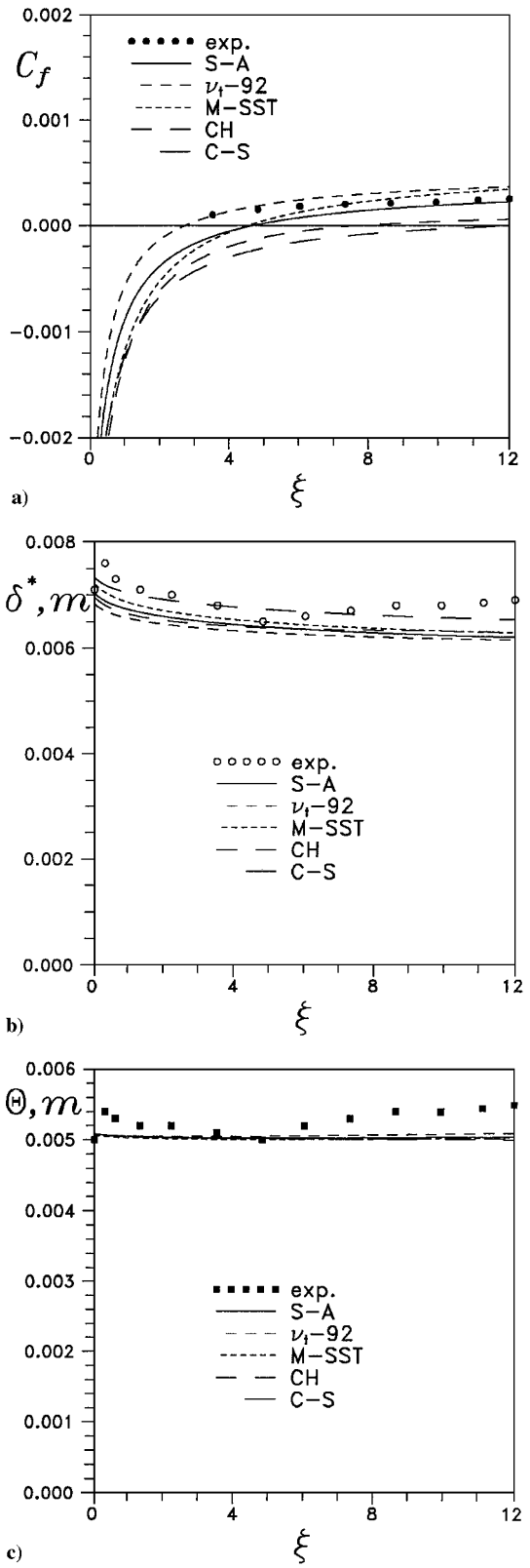

Fig. 3 Streamwise distributions of a) skin-friction coefficient, b) displacement thickness, and c) momentum thickness.

end of the stationary plate, just before the start of the perturbation. The parameter $\xi = (x - x_0)/\delta_0$ in Fig. 2a is the normalized form of the streamwise coordinate, x_0 is the location of the leading edge of the moving belt, and δ_0 is the boundary-layer thickness there. One can see that all of the models, except perhaps for the C–S model, give velocity profiles rather close to each other and to the experimental one. The observed discrepancy can be attributed, at least partially, to the fairly low Reynolds number at the end of the stationary plate: $Re_\Theta \cong 2 \times 10^3$. The turbulence might not be completely developed in the experiment, and this Reynolds-number range is not emphasized in the calibration of the models ($Re_\Theta = 1 \times 10^4$ is typical). However, that discrepancy is not too high, which supports the claim in Ref. 1 that, though the flow is not quite free of low-Reynolds-number effects, they do not seem to be significant. This conclusion can be drawn also on the basis of the comparison of the computed $C_f(Re_\Theta)$ curves, with the corresponding experimental data and the well-known Karman–Schoenherr and Bradshaw correlations for a flat plate turbulent boundary layer (Fig. 2b).

Figure 3 shows the comparison of the models' predictions with the experimental data on the streamwise distributions of the skin-friction coefficient C_f and boundary-layer integral thicknesses (δ^* and Θ) along the moving all. All of the models do predict the crucial drop and sign change of the friction coefficient observed in the experiment, beginning between $\xi = -0.3$ and $+0.3$ and extending to $\xi = 3$. With the M-SST, S–A, and ν_t-92 models, just as in the experiment, after that drop, C_f becomes positive again and then increases gradually while remaining around an order of magnitude smaller than on the stationary plate; it is very close to the experimental data. The k–ε Chien and C–S models, unlike the M-SST, S–A, and ν_t-92 models, fail to predict the positive C_f values observed in the experiment over the major part of the moving belt. Thus, we observe that from the friction prediction standpoint the M-SST, S–A, and ν_t-92 models can be evaluated as unexpectedly good and having a significant advantage over the C–S and Chien models. This is less of a disappointment for the C–S model because algebraic models were not claimed to respond well to step changes of the boundary conditions.

With regard to the displacement and momentum thicknesses predictions with different models, their disparity at the moving belt is even less than that observed at the still plate and, in general, the models agree with the data quite well (Figs. 3b and 3c). The experimental friction and momentum-thickness distributions are not perfectly consistent with the von Kármán momentum equation: the derivative $d\Theta/dx$ changes its sign at $\xi \cong 5.0$ (Fig. 3c) while the friction coefficient becomes positive tangibly earlier, at $\xi \cong 2.0$ (Fig. 3a). The absolute value of the derivative also seems to be high, when compared with the friction coefficient.

One of the major findings of Ref. 1 is that, in spite of the significant decay of the turbulent shear stresses in the inner layer caused by the abrupt change of the slip velocity from zero to that of the moving belt, the structure of the outer region of the disturbed boundary layer is little affected by this decay. It remains virtually unaltered at least as far along the moving belt as 10 initial boundary-layer thicknesses. It appears that with any of the considered models the computed velocity profiles demonstrate just the same behavior. One can see this from Fig. 4, where the evolution of the velocity profiles computed with different models is presented. Though the velocity profiles with different models are rather different (their comparison with the experimental data is considered, in Fig. 5), the perturbation to the initial velocity profiles generated by all of the differential models at $\xi = -0.3$ remains restricted to the vicinity of the wall, and even at the last experimental station ($\xi = 11.1$) it reaches only around $y/\delta_{99} = 0.3 \sim 0.4$ (Fig. 4), which agrees fairly well with the experiment (δ_{99} is the local boundary-layer thickness). With the algebraic C–S model, the reaction of the outer layer to the perturbation of the inner one starts somewhat earlier, but is not very strong either.

We view this result as more predictable than the authors of Ref. 1 did. A fair timescale for the outer layer is δ/u_*, or here about $25 \cdot \delta/U_e$; u_* is the friction velocity on the fixed plate and sets the scale for the incoming turbulence. The time for outer-layer eddies to travel a distance of $x = 10\delta$ ($\xi = 10$) is about $13 \cdot \delta/U_e$; therefore, a full adjustment to the new near-wall input cannot be expected. An additional factor is that the near-wall turbulent eddies, which are altered, have length scales much smaller than those of the outer eddies; this impedes the propagation of the alteration. A further factor is that the altered eddies are weakened, relative to those in the outer layer. To check this estimation (while not claiming that models contain all of the physics), computations were performed for a very long moving belt (ξ up to 1000). The results presented in Fig. 4f show that with the S–A model, the outer region of the boundary layer

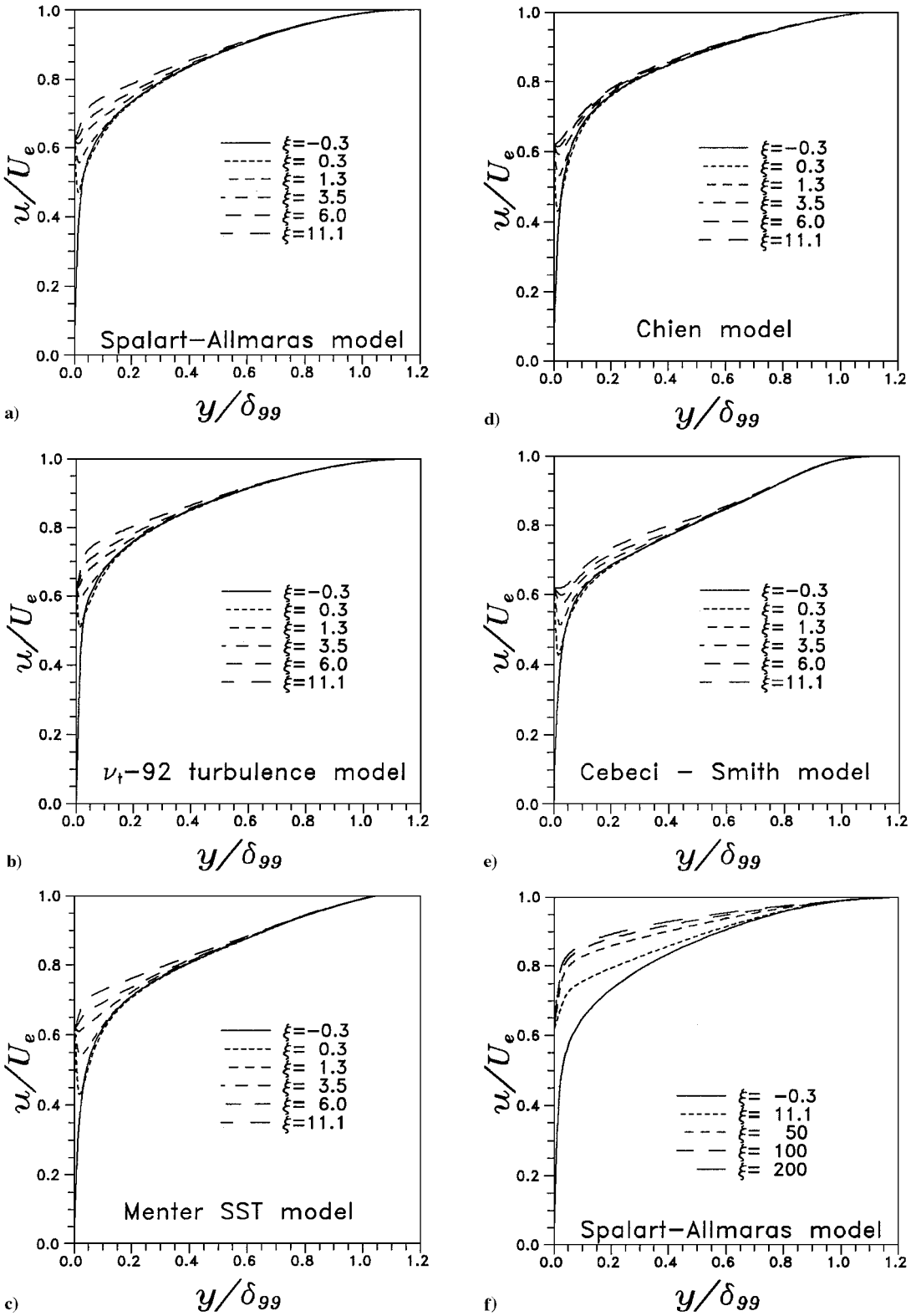

Fig. 4 Evolution of the streamwise mean velocity profiles along the moving belt ($\xi \leq 11.3$) computed with different turbulence models and S–A predictions up to $\xi = 100$.

at the moving belt can be considered as fully developed only as far downstream from the beginning of the belt as $\xi \cong 100$. Very similar results were obtained with the other turbulence models.

Thus, we can conclude that from the standpoint of the slight response of the velocity profile in the outer layer to the sudden inner-layer removal, all of the turbulence models we have considered perform quite well. Let us now consider the correspondence between the models' predictions and the experimental data in more detail.

Figures 5 and 6 contain a comparison of the computed and measured mean velocity and Reynolds shear-stresses profiles evolution along the moving belt. One can see that the computed velocity profiles in the close vicinity of the leading edge of the belt exhibit too rapid a relaxation. For instance, at the first experimental station $\xi = 0.3$ the measured minimum value of u/U_e is around 0.35, whereas the corresponding computed values lay in the range $0.42 \sim 0.5$ (Fig. 5a). Then that discrepancy gradually decreases (Figs. 5b–5e), and in the later-response region ($\xi \geq 3.5$), the velocity profiles in the inner layer computed with the use of the S–A and, especially, with the M-SST model agree well with the experiment; the ν_t-92 model somewhat overestimates the rate of inner-layer

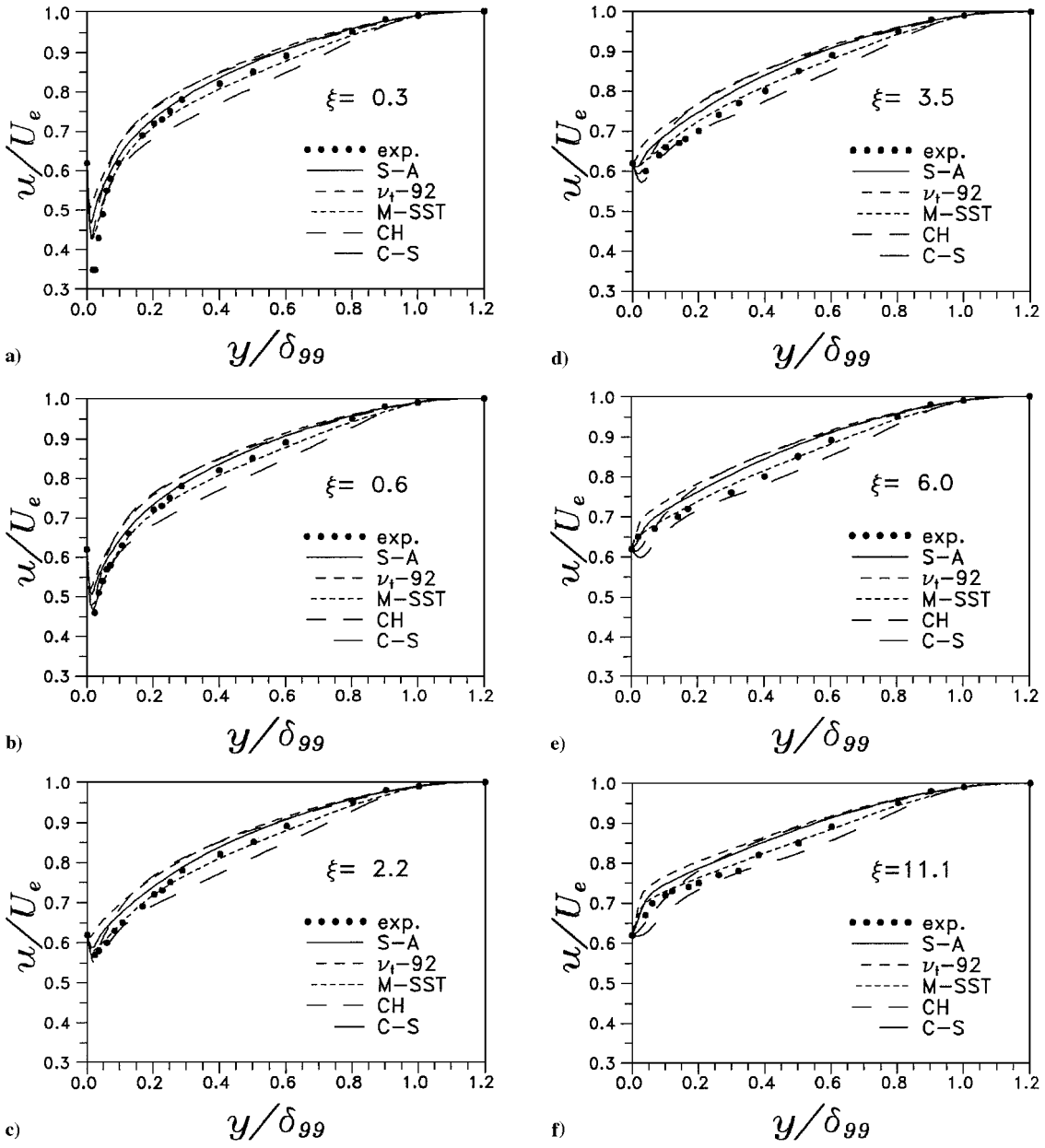

Fig. 5 Comparison of measured and computed streamwise mean velocity profiles.

relaxation, whereas the Chien and, especially, C–S models, on the contrary, tangibly underestimate that rate, which results in very low (and even negative) skin friction at the moving belt as already mentioned. Thus, an adequate prediction of the velocity relaxation in the inner region of the boundary layer turns out to be an issue for all of the turbulence models, though the M-SST model experiences difficulties mostly at the stage of the flow initial response ($\xi \leq 3.5$), whereas the other models disagree with the data to varying degrees up to the end of the moving belt ($\xi = 11.1$; see Fig. 5f).

A similar conclusion applies to the Reynolds shear stress profiles (Fig. 6). Just as for the velocity profiles, no model is able to predict the experimental data in the inner layer in the initial response region (all of the models significantly underestimate the stresses). In the later-response region ($\xi \geq 3.5$), the predictions of the stress profiles provided by the S–A, M-SST, and ν_t-92 models are close to each other and to the experiment (Figs. 6a–6c). This is a pleasant surprise because they have not simply returned to the standard shape of the flat plate boundary layer. The Chien and C–S models significantly underestimate the stresses everywhere at the moving belt (Figs. 6d and 6e), and it seems that the Chien model demonstrates a very strong effect of diffusion coming from the wall region. This effect is probably caused by the action of the damping function introduced in the Chien model to describe low Reynolds number effects.

To summarize, the results obtained give solid evidence of the superiority of the M-SST, S–A, and ν_t-92 models over the Chien and C–S models. As to the inability of the first three models to describe very accurately the inner-layer response to the sudden slip velocity increase, at least two explanations could be suggested. The first one is associated with the effect of the extra (stretching) strain caused by the jump of the wall velocity. According to the experiment, this results in a significant growth of the Reynolds-stress components in the region of initial response (Fig. 6), which cannot be accounted for properly by the eddy-viscosity turbulence models with which we are dealing. The second proposal is the additional inaccuracy introduced by the approximate approach used in the computations to describe the effect of the extra mass $\dot{m}$ dragged through the gap between the stationary plate and the moving belt, which, apparently, shall have the strongest influence exactly in the initial response region. To evaluate the role of the vagueness in the $\dot{m}$ value, a series of computations was performed with that parameter varying from $\dot{m} = 0$ up to $\dot{m} = 0.03$ of the total mass flux across the boundary layer. The corresponding results obtained with the S–A model are presented in Fig. 7. (Other models react to the variation of $\dot{m}$ quite similarly.) One can see from Fig. 7 that the $\dot{m}$ value affects the results quite tangibly and that increasing it up to 3% of the mass flux through the boundary layer results in a better prediction of both

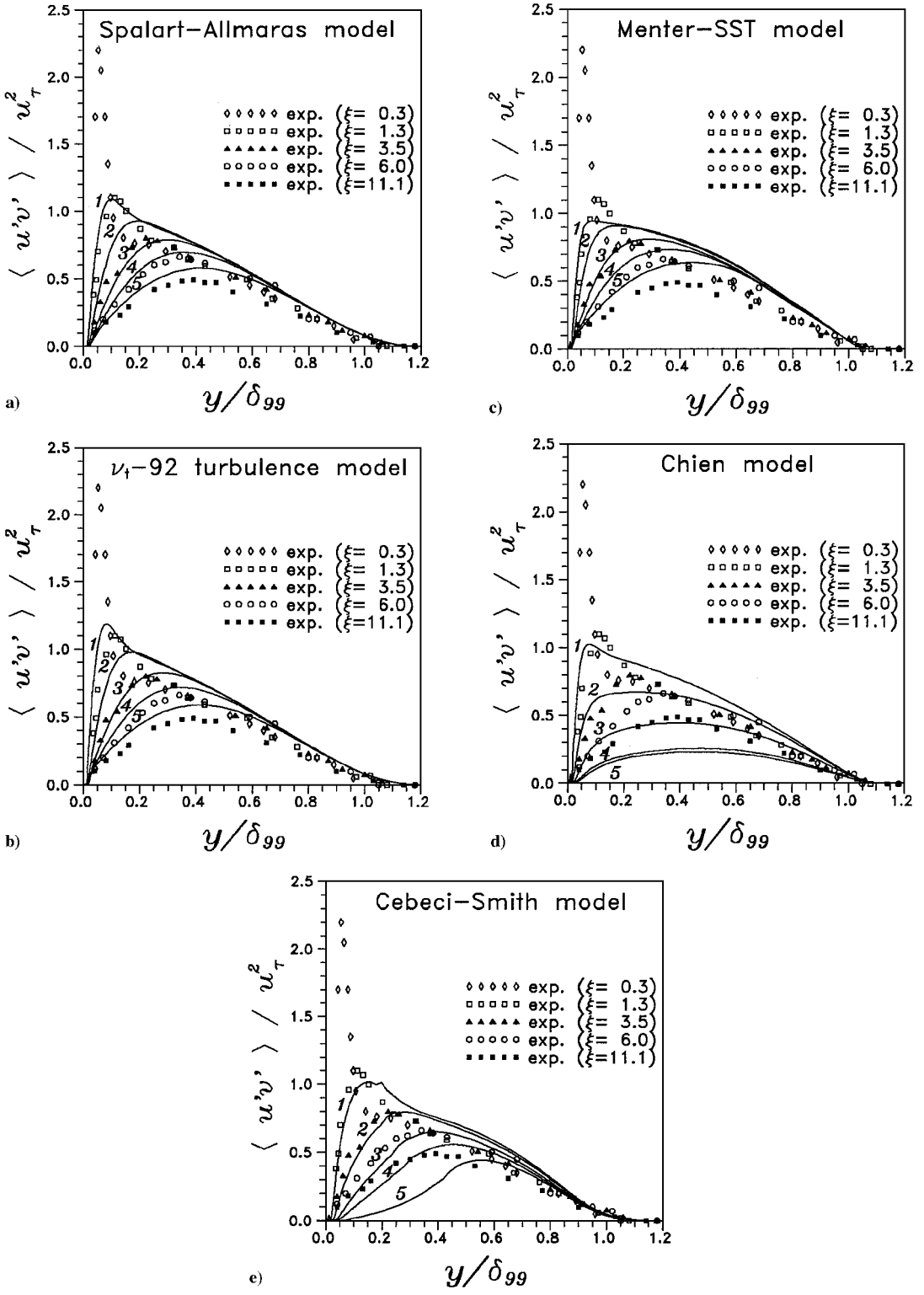

Fig. 6 Comparison of measured and computed Reynolds shear stress profiles at $\xi = 0.3, 1$; $\xi = 1.3, 2$; $\xi = 3.5, 3$; $\xi = 6.0, 4$; and $\xi = 11.1, 5$.

velocity and shear stress profiles in the region of initial response. However, in the later-response region, it makes the agreement with the data somewhat worse. Thus, we can conclude that the approximate modeling of the moving belt effect used in the computations (prescribing a linear variation of the streamwise velocity and constant, with $\dot{m} = 1\%$, normal velocity along the gap) might bear some responsibility for the insufficient accuracy of the S–A, ν_t-92, and M-SST in the initial-response region.

Figure 8, related to the H–A flow, shows the models' performance over the stationary plate placed downstream of the moving belt. It shows that, just as in the experiment, the response of all of the models to the sudden return of a high shear stress in the inner region, unlike their reaction to its removal, is very fast. In other words, all of the models predict the nonreversibility of the boundary-layer response to the removal vs restoration of the mean shear found in the experiment. This is consistent with our earlier argument that weakened turbulence in one region is not as prompt in propagating changes as strengthened turbulence is.

D–H Flow

The major feature of interest found in the experiment[2] is the lack of alignment of the Reynolds stresses and the mean shear in the x–z plane. We were ready for a similar and inadequate behavior of scalar eddy-viscosity turbulence models, including those studied in the

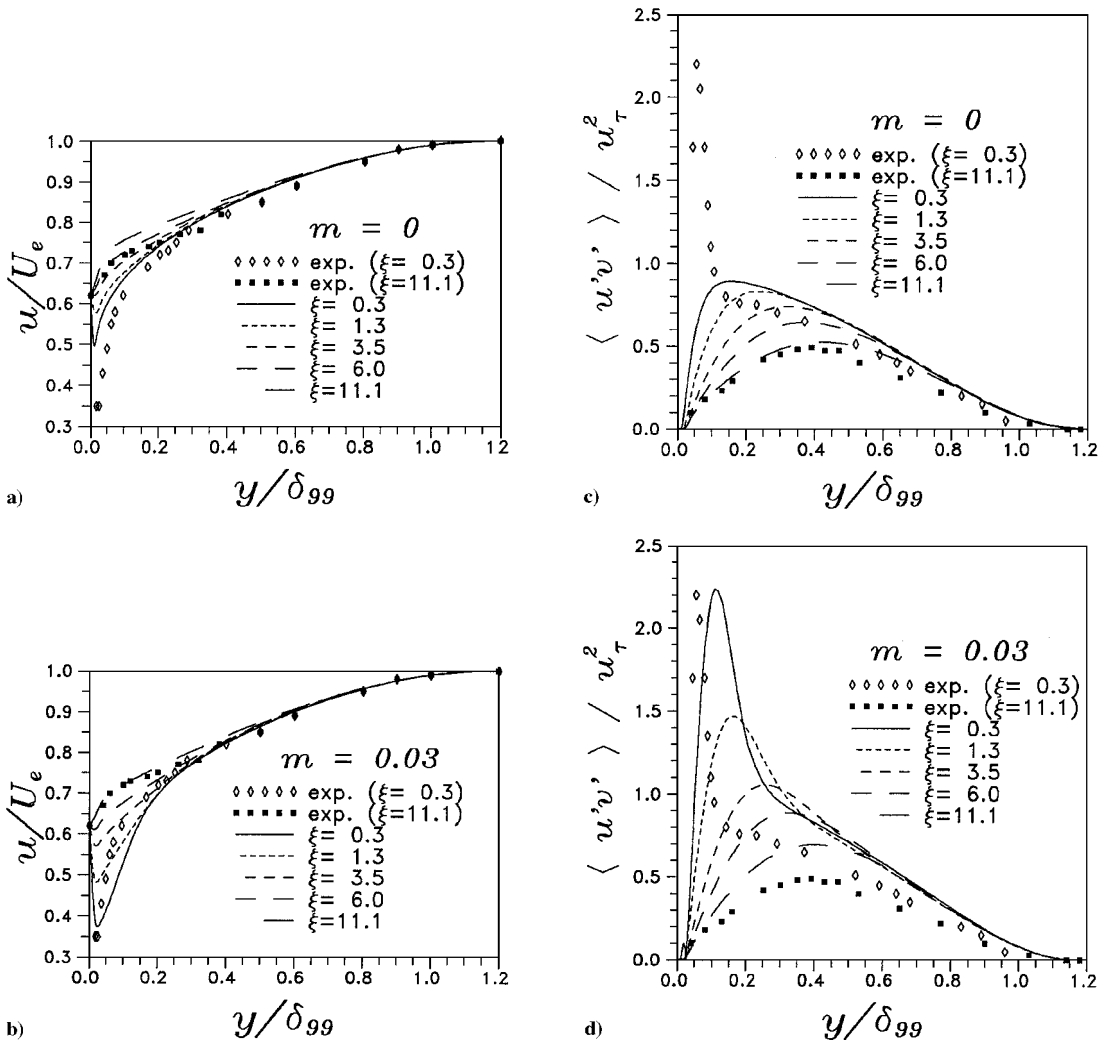

Fig. 7 Effect of additional mass flux injected through the gap on the computed mean velocity and Reynolds shear stress profiles due to the S–A model.

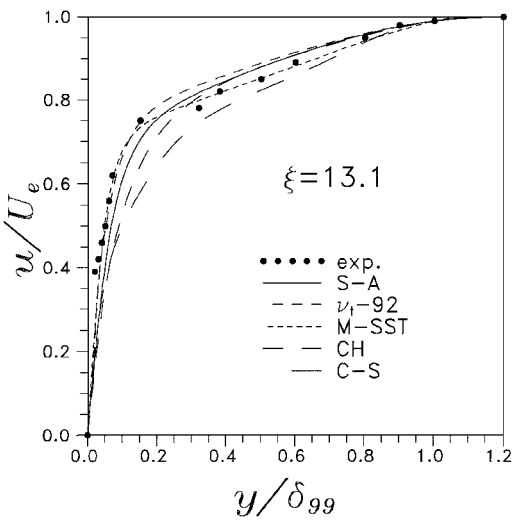

Fig. 8 Computed and measured mean streamwise velocity profiles at the stationary flat plate downstream of the moving belt.

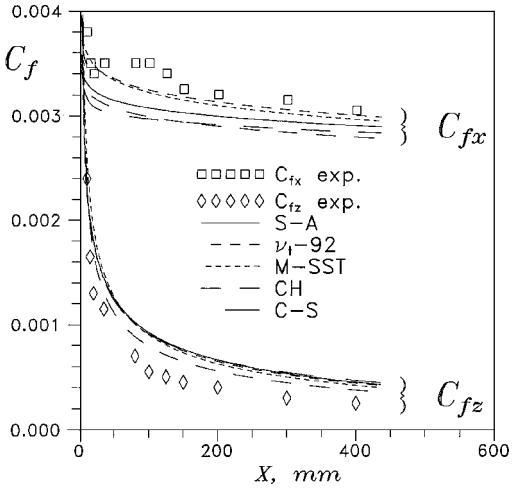

Fig. 9 Comparison of the computed and measured axial and transverse skin-friction coefficients distributions downstream of the spinning cylinder.

present work. However, as it often occurs with turbulence models, they do not perform as badly as could be expected, as shown by their agreement with the experimental data on the major mean flow characteristics in Figs. 9–12.

We first find that the longitudinal distributions of both axial and transverse skin-friction coefficients C_{fx} and C_{fz} compare fairly well with the experiment (Fig. 9). The latter quantity demonstrates a rapid drop caused by the decrease of the transverse velocity downstream of the spinning cylinder, just as observed in the experiment. The axial mean velocity profiles u/U_e, in general, also agree with the experimental data quite acceptably (Fig. 10a), although the models do not predict the small flow acceleration seen near the wall in the experiment.

The agreement of the transverse mean flow characteristics with the data is somewhat worse than that of the streamwise flow. Namely, the flow angle β in the vicinity of the wall in the computations turns

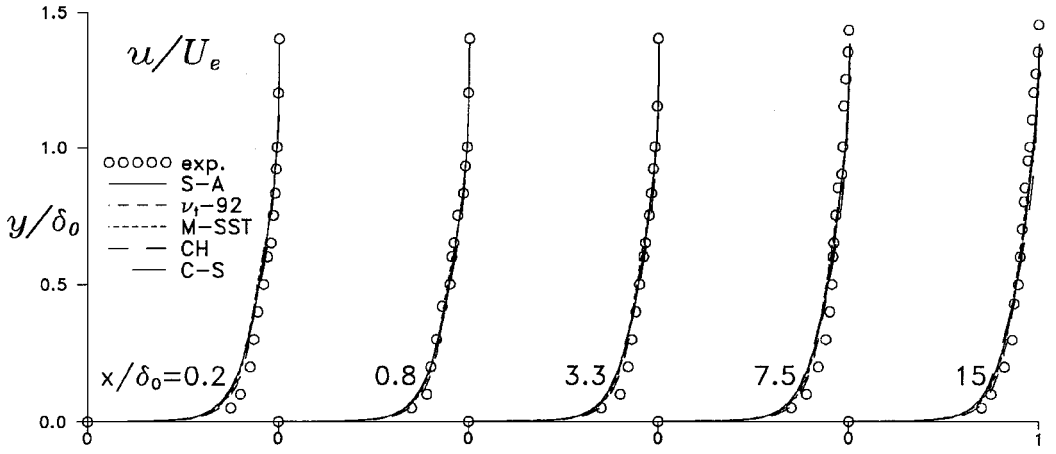

a) Axial mean velocity

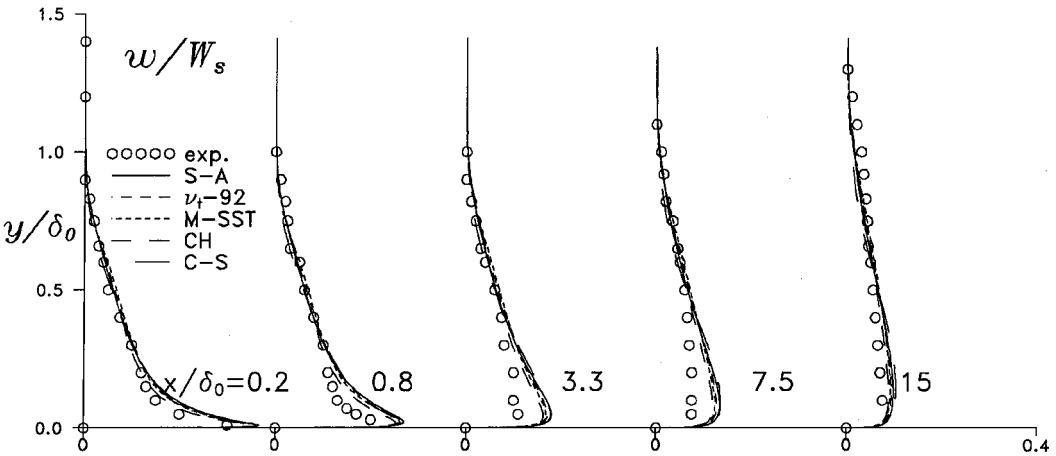

b) Transverse mean velocity

Fig. 10 Comparison of the measured and computed profiles downstream of the spinning cylinder.

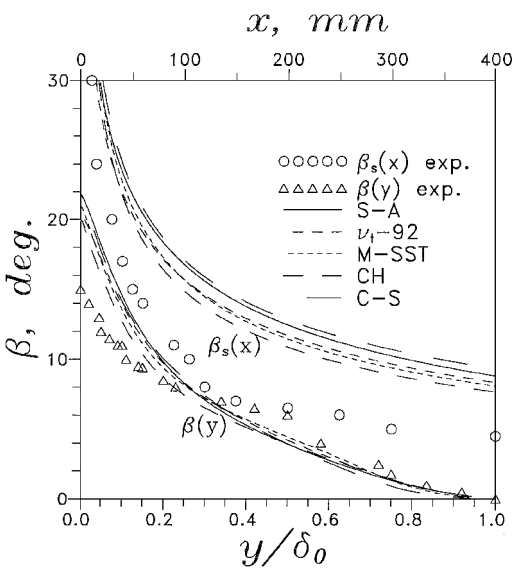

Fig. 11 Computed and measured streamwise distributions of the surface flow angle $\beta_s(x)$ and flow-angle profile $\beta(y/\delta_0)$ at $x/\delta_0 = 1.7$.

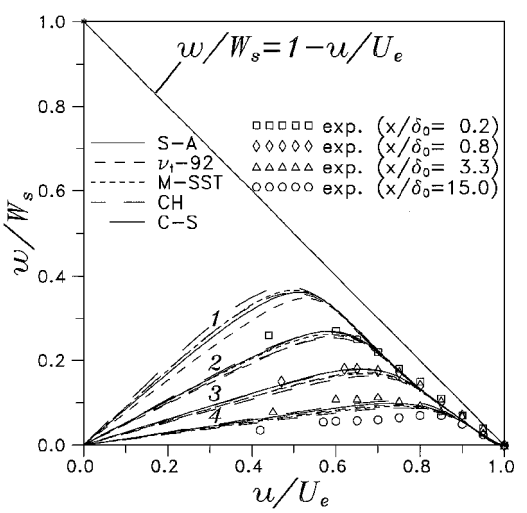

Fig. 12 Polar velocity plots: models' predictions at $x/\delta_0 = 0.2$, 1; $x/\delta_0 = 0.8$, 2; $x/\delta_0 = 3.3$, 3; and $x/\delta_0 = 15.0$, 4.

out to be tangibly overestimated. That inaccuracy of the models can be seen from the comparison of the models' predictions with the experimental data on the streamwise distribution of the surface flow angle and from the flow-angle profile at $x/\delta_0 = 1.7$ shown in Fig. 11. Therefore, we can conclude that the models significantly underestimate the rate of decay of the transverse velocity w nearest the wall as also clearly seen from Fig. 10b, where the evolution is shown of the computed and measured transverse velocity profiles. However, the outer part of the transversal velocity profiles is predicted rather accurately. The same trends are shown in another form in Fig. 12, where the evolution is presented of a polar velocity plot downstream of the spinning and stationary cylinders junction.

Note also that the character of the discrepancy between the models' predictions and the experimental data for the D–H mean flow is not the same as that for the H–A flow. In particular, as was already mentioned, for the D–H flow all of the models underestimate the rate of response of the transverse velocity in the near-wall region to the new boundary condition (cessation of spin), whereas for the H–A

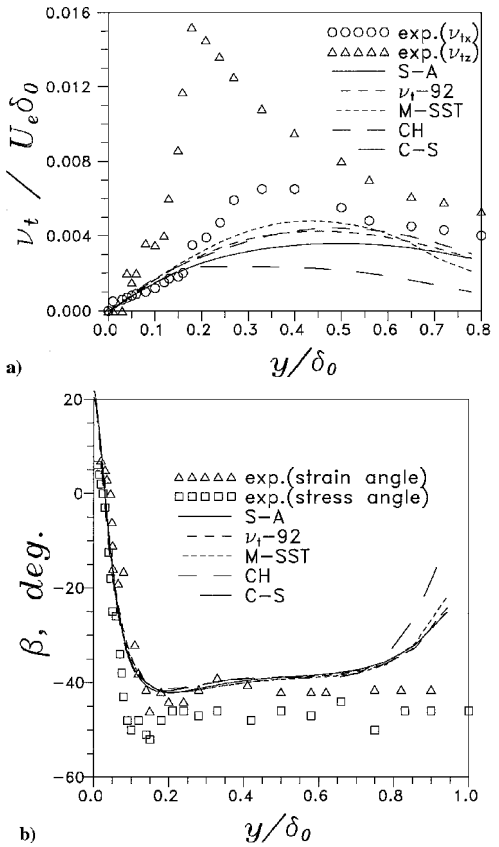

Fig. 13 Experimental data on ν_{tx}, ν_{tz}, and strain and stress angles compared with a) computed scalar eddy viscosity and b) strain/stress angle profiles.

flow they, on the contrary, overestimate the rate of the inner-layer response to the abrupt increase of the slip velocity (Fig. 5). Also note that for the H–A flow the discrepancy between the predictions and the data on the mean velocity is gradually decreasing downstream of the perturbation location, whereas for the D–H flow that discrepancy is first growing and then starts dropping only at $x/\delta_0 \geq 7.5$ (Fig. 10b). This difference is probably explained by the different sources of the models deficiency for the two flows being considered. In the H–A flow, we have invoked the memory effects and an additional stress generation due to the strong flow acceleration in the close vicinity of the gap between the stationary plate and moving wall; both factors have a diminishing influence downstream of the gap. In the D–H flow, the major source of the models inaccuracy is the violation of the scalar eddy-viscosity assumption, which, based on the experiment, is negligible at the spinning cylinder but becomes rather severe downstream, that is, exactly where the maximum disagreement is observed between the predictions and the data on the transverse velocity. The level of difference between the streamwise and transverse eddy-viscosity components ν_{tx} and ν_{tz}, determined in the experiments as the ratios of the appropriate shear stress and strain components at $x/\delta_0 = 3.3$, is shown in Fig. 13a; the computed, scalar, eddy viscosity profile is also presented. One can see that the models' predictions more or less agree with the data on ν_{tx} and crucially, by a factor of 4, underestimate the data on ν_{tz}. This makes it quite clear why the computations predict too slow a decay of the transverse flow. The same effect is shown in Fig. 13b, where a comparison is presented of the experimental strain and stress angles with a corresponding computed profile (in the framework of the scalar eddy-viscosity models, the angles are identical).

In general, the turbulent characteristics computed with the different turbulence models for the D–H flow are far from satisfactory, which is just what could be expected for a flow with significant spread between Reynolds-stress and strain directions. Curiously, whereas the scalar eddy viscosity ν_t predicted by the models agrees better with the experimental axial eddy viscosity ν_{tx}, for the shear

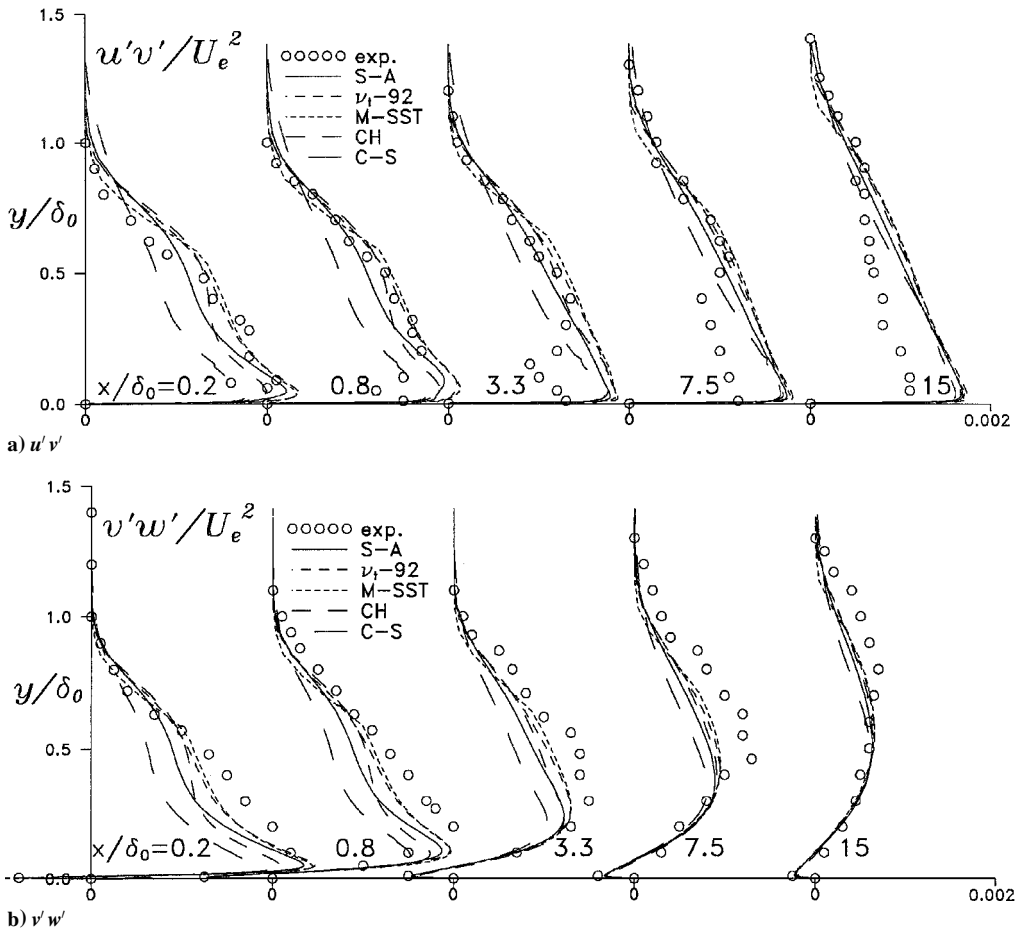

Fig. 14 Comparison of the measured and computed Reynolds shear stress.

stresses, a qualitatively better correspondence is observed for the transverse component $u'w'$. As shown in Fig. 14, the measurement reveals a local minimum in the $u'v'$ profiles whereas the models predict a maximum near the wall where the data has a minimum (note that computations with the use of the Launder et al.[11] Reynolds stress model performed in Ref. 2 have just the same defect). Computed and measured transverse shear stress profiles (Fig. 14b) are qualitatively similar though all of the models tangibly underpredict the measured $u'w'$ values.

As to the models' rating, it differs in the D–H flow and in the H–A flow. The most evident difference is that for the D–H flow all of the models perform almost the same, and no significant superiority is observed of the M-SST, S–A, and ν_t-92 models over the k–ε Chien model (recall that for the H–A flow the latter one is definitely lagging). Only the simplest algebraic C–S model gives tangibly worse results than all of the others, especially for the turbulent flow characteristics.

Conclusions

Two boundary layers with an abrupt change of the wall velocity have been studied numerically with the use of several eddy-viscosity turbulence models. From the comparison of the models' predictions with the experimental data for the first flow (H–A)[1] it can be concluded that the one-equation eddy viscosity transport turbulence models, S–A[5] and ν_t-92 (Ref. 6), and the two-equation k–ω SST model[8] are quite capable of predicting the major flow characteristics everywhere except for the close vicinity of the gap between the stationary plate and the moving belt used in the experiment to implement a sudden removal of the inner region of the boundary layer. The Chien[7] k–ε model, just as the simple algebraic mixing-length C–S model,[10] turned out to be unable to predict this flow accurately.

As could be expected, eddy-viscosity models are unable to capture the turbulent flow characteristics directly associated with the Reynolds-stress vector direction, which is rather significant for the three-dimensional boundary layer on the spinning/stationary cylinder system studied experimentally (D–H).[2] However the major mean flow characteristics (for instance, the skin-friction distribution and the axial and transverse velocity profiles) computed with the differential models do not suffer from that drawback as much as we expected and are computed with a sufficient accuracy. Possibly, the inner layer has much control over the skin friction and does not contain protracted three-dimensional effects.

A general conclusion based on both flows is that the response of the k–ω SST model and the S–A and ν_t-92 one-equation models to an abrupt change of the wall velocity is qualitatively correct and, by and large, accurate. The Chien k–ε model performed well only in one flow; the algebraic C–S model, as could be expected because it was meant for slowly evolving flows, failed to predict either flow correctly.

Acknowledgments

Funding for this work was provided by Boeing Operations International, Inc., and, partially, by the Russian Basic Research Foundation (Grant 97-02-16492).

References

[1]Hamelin, J., and Alving, A. E., "A Low-Shear Turbulent Boundary Layer," *Physics of Fluids*, Vol. 8, No. 3, 1996, pp. 789–804.

[2]Driver, D. M., and Hebbar, S. K., "Experimental Study of a Three-Dimensional, Shear-Driven, Turbulent Boundary Layer," *AIAA Journal*, Vol. 25, No. 1, 1987, pp. 35–42.

[3]Bissonnette, L. R., and Mellor, G. L., "Experiments on the Behavior of an Axisymmetric Turbulent Boundary Layer with a Sudden Circumferential Strain," *Journal of Fluid Mechanics*, Vol. 63, Pt. 2, 1974, pp. 369–413.

[4]Higuchi, H., and Rubesin, M. W., "Behavior of Turbulent Boundary Layer Subjected to Sudden Transverse Strain," *AIAA Journal*, Vol. 17, No. 9, 1979, pp. 931–941.

[5]Spalart, P. R., and Allmaras, S. R., "A One-Equation Turbulence Model for Aerodynamic Flows," *La Recherche Aérospatiale*, No. 1, 1994, pp. 5–21.

[6]Shur, M., Strelets, M., Zaikov, L., Gulyaev, A., Kozlov, V., and Secundov, A., "Comparative Numerical Testing of One- and Two-Equation Turbulence Models for Flows with Separation and Reattachment," AIAA Paper 95-0863, Jan. 1995.

[7]Chien, K. Y., "Predictions of Channel and Boundary-Layer Flows with a Low-Reynolds-Number Turbulence Model," *AIAA Journal*, Vol. 20, No. 1, 1982, pp. 33–38.

[8]Menter, F. R., "Zonal Two-Equation k–ω Turbulence Models for Aerodynamic Flows," AIAA Paper 93-2906, July 1993.

[9]Bardina, J. E., Huang, P. G., and Coacley, T. J., "Turbulence Modeling Validation," AIAA Paper 97-2121, 1997.

[10]Cebeci, T., "Calculation of Three-Dimensional Boundary Layers, Part 1: Swept Infinite Cylinders and Small Crossflow," *AIAA Journal*, Vol. 12, No. 6, 1974, pp. 779–786.

[11]Launder, B. E., Reece, G. J., and Rodi, W., "Progress in the Development of a Reynolds-Stress Turbulence Closure," *Journal of Fluid Mechanics*, Vol. 68, Pt. 3, 1975, pp. 537–566.

C. G. Speziale
Associate Editor